IET Microwaves, Antennas & Propagation

Research Article

IET Journals
The Institution of Engineering and Technology

Compact UWB FSS reflector for antenna gain enhancement

ISSN 1751-8725
Received on 28th January 2019
Revised 21st March 2019
Accepted on 28th March 2019
E-First on 1st May 2019
doi: 10.1049/iet-map.2019.0083
www.ietdl.org

Yanning Yuan[1], Xiaoli Xi[1] ✉, Yuchen Zhao[1]

[1]*The Faculty of Automation and Information Engineering, Xi'an University of Technology, Shaanxi, Xi'an, People's Republic of China*

✉ *E-mail: xixiaoli@xaut.edu.cn*

Abstract: In this study, two compact ultra-wideband (UWB) frequency selective surface (FSS) reflectors, which combine the branch loading method with the design of the traditional FSS, are proposed for antenna gain enhancement application. The working mechanism of the proposed FSS reflectors is analysed by the equivalent circuit model. The first FSS reflector, which is a 10 × 10 array with 8.25 mm × 8.25 mm unit size, not only enhances the gain of the UWB antenna, but also guarantees a constant gain with only 0.5 dB variation across the whole operation band. To further reduce the reflector size, a more compact FSS reflector with 6.25 mm × 6.25 mm unit size is designed by printing similar patterns on both sides of a single-layer dielectric slab. Compared to the first structure, the second reflector can realise a 25% size reduction and the same gain variation in the entire UWB frequency range. The only compromise is a 0.5 dB gain decrease. Finally, a good agreement between the measured and simulated results proves the feasibility of the authors' design.

1 Introduction

In the past decade, ultra-wideband (UWB) applications in various fields have attracted wide attention [1]. As a radiator commonly used in UWB systems, monopole antennas have an omnidirectional and bidirectional radiation pattern in their principal radiating planes [2, 3]. The disadvantage of this type of antenna is that the main lobe gain is low, the back radiation is large, and it is susceptible to the surrounding environment. Frequency selective surface (FSS) reflector with an UWB band-stop response and a linearity decreasing phase can improve the directionality and the gain of the antenna, and weaken the influence of the installation environment on its characteristics (reduced back-lobe radiation) [4, 5]. Owing to its unique frequency selection characteristics, frequency selection surface has also attracted the attention of scholars in other fields and is widely used in filters [6, 7], radar scattering [8], radio-frequency identification [9], compact antenna array decoupling [10, 11], and other fields. To achieve certain specific design purposes, some existing design methods have also been introduced into FSS design such as fractal [12, 13], metamaterial [14], artificial magnetic conductor (AMC) structure [15, 16] etc.

To obtain an UWB response, the multi-layer stacks FSS structure with different frequency responses are used in [4, 14, 17–19]. In [17], the reflection phase changes linearly, and the gain increases by 4–5 dB in the UWB frequency range are obtained by a three-layer FSS structure. In [18, 19], the UWB slot antenna loaded with a four-layer FSS reflector is used to improve the gain in the whole UWB band, and the gain variation is only 0.5 dB in [19]. Furthermore, several double-layer FSS structures are presented in [4, 14]. The two-layer FSS reflector, which is a 5 × 13 array with 22.4 mm × 6.5 mm unit size, is described in [4] to increase the gain in the entire UWB band by ∼3–4 dB, but the gain varies greatly (about 7 dB). In [14], the metamaterial is used to realise miniaturised FSS design. After the antenna is loaded, the gain is enhanced by 3–4 dB, and the group delay is nearly constant. At the same time, its radiation pattern in the *H*-plane is almost omnidirectional. The stacking method, though quite effective, still suffers from several drawbacks including the difficulty of design and debugging, the cost of product processing, and the large structure size. As a result, the multi-layer structure is not suitable for low profile, compact antenna design. Moreover, achieving a flatter gain variation is also a critical point in such a wide operating frequency range.

Recently, some single-layer FSS reflectors are designed to achieve constant gain in the UWB band [5, 20, 21]. In [5], the basic square ring and circular ring are used to realise the stop-band response characteristics. By changing the dielectric constant of the dielectric material, the miniaturisation design of FSS is realised, and both of them have obtained the quasi-constant gain. Yahya *et al.* [20] provide an FSS design method similar to the high-impedance surface characteristics. Loading the FSS reflector, the average gain of a coplanar waveguide (CPW) antenna is 9 dBi, and the variation range is only 0.5 dB. Yahya and Itami [21] utilise the high response frequency aperture elements to obtain fading reflective characteristics (high-pass response). This method provides a good FSS design guidance for improving the low-frequency gain of the antenna.

In this paper, two compact FSS reflectors printed on a single-layer slab are proposed to exhibit desired reflection and linear phase variation characteristics in the entire UWB band. The unit size of the first FSS reflector is 8.25 mm × 8.25 mm, <1/10th of the working wavelength (corresponding frequency 3 GHz). Moreover, this reflector, which is a 10 × 10 array, is used to load a CPW UWB antenna to achieve the 8.5 dBi average gain and 0.5 dB gain variation in the whole UWB bandwidth (BW). On this basis, a more miniaturised FSS reflector is presented by printing similar structure on both sides of a single dielectric slab with an array size of 62.5 mm × 62.5 mm. After loading the second FSS reflector, the gain of the antenna decreases by only 0.5 dB compared with the original reflector, and the gain variation is still 0.5 dB in the whole UWB band. At the same time, the loading of the two reflectors does not degrade the time-domain impulse response characteristics of the antenna. The design and optimisation process has been performed using CST Microwave Studio. The working mechanism of FSS is explained by the equivalent circuit model (ECM). The good agreement between the simulated and measured results demonstrates the validity of our designs.

This paper is organised as follows. Section 2 describes the antenna design, the FSSs unit design, the antennas loaded proposed FSSs, as well as time-domain simulation. In Section 3, the designed antenna and FSS unit are processed and tested, and the simulation and test results are compared. Finally, the conclusions are drawn in Section 4.

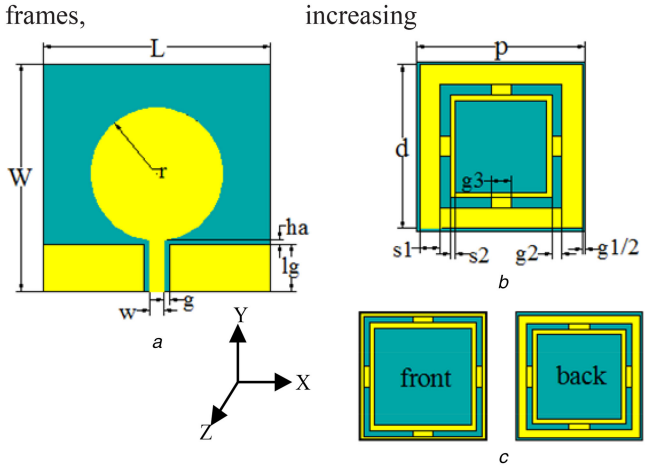

Fig. 1 *Structure of the proposed UWB antenna and FSSs unit*
(a) Antenna, ***(b)*** FSS1, ***(c)*** FSS2

Table 1 Dimensions of the proposed UWB antenna (millimetres)

Variable	*L*	*W*	*r*	*w*	*g*	*ha*	*lg*
value	50	50	14.5	3	0.28	0.5	11

Table 2 Dimensions of the proposed FSS (millimetres)

	p	*d*	*s1*	*s2*	*g1*	*g2*	*g3*
FSS1	8.25	8	1	0.25	0.25	0.5	1
FSS2 front	6.25	6.15	0.15	0.25	0.1	0.3	1
FSS2 back	6.25	6	0.40	0.25	0.25	0.3	1

2 Design process and simulation results

2.1 Antenna design

To evaluate the performance of the designed FSS, the CPW-fed circular-disc monopole antenna, which the original design is derived from [2], and the model is also used as a radiator in [20, 21]. In this paper, the CPW-fed circular-disc monopole antenna is printed on Rogers RO4350B substrate of the dielectric constant of 3.48 and thickness of 1.524 mm. The used radiator is shown in Fig. 1*a* and final dimensions are given in Table 1.

2.2 FSS1 design

The performance of FSS mainly depends on geometry, element size, element spacing, dielectric thickness, electrical characteristics, the incident angle of the excitation wave etc. Through the basic EC, we can see that the geometry of the cell determines the type of the filter. The patch FSS impedance is capacitive, and the band-stop characteristic can be realised when the frequency of the incident wave is the same as its resonance frequency. 'Ring' element can be regarded as evolved from the dipole element, and its resonance stability is better when the electromagnetic (EM) wave with different incident angles and polarisation is incident. So the new compact single-layer UWB stop-band FSS1 designed in this paper contains two basic square ring resonant elements: outer and inner, as shown in Fig. 1*b*. Since the two radiation elements are not connected and their lengths are different, they resonate with different frequencies and form two independent operating bands. With loading four branches between each other, the working BW is expanded. In other words, this paper combines the branch loading method with the design of the traditional FSS, adding four adjustment branches in two traditional square frames, increasing the electrical size of the entire patch, thereby increasing the current loop and extending the impedance BW. The FSS structure designed in this paper is printed on the dielectric substrate of Rogers RT6010, which the relative dielectric constant is 10.2 and the thickness is 0.635 mm. The parameters of the optimised FSS1 unit are shown in Table 2.

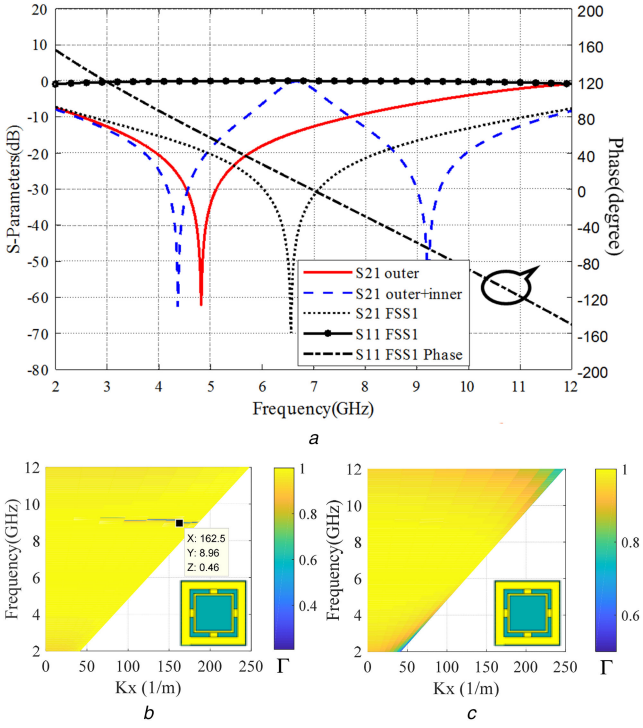

Fig. 2 *S-parameters and dispersion diagram of FSS1*
(a) S-parameters, ***(b)*** Dispersion diagram at TE mode, ***(c)*** Dispersion diagram at TM mode

Through the analysis of the response of each component of the unit structure in the wide spectrum, it can be seen from Fig. 2*a* that the resonant frequency of a single outer square ring is 4.9 GHz. Owing to the length and width of the outer ring directly affect the low-frequency characteristics of FSS, the design of the outer ring emphasises satisfying the low-frequency characteristics. Similarly, the design of the inner ring meets the high-frequency characteristics. Since the inner and outer loops are disconnected from each other, they exhibit independent narrowband response. Owing to the coupling effect each other, the low-frequency response frequency shifts slightly from 4.9 to 4.4 GHz, and the high-frequency response is 9.2 GHz. Through branch loading, the return loss in the entire UWB frequency band is lower than the industry standard −10 dB, that is, it has a good high attenuation stop-band characteristic in the 3–11 GHz frequency band.

To achieve a high-gain FSS loading antenna, the reflection phase of the FSS should satisfy the resonance condition over a wide-frequency range. It can be seen from Fig. 2*a* that the phase of the designed FSS1 unit varies linearly with frequency, that is, a different frequency corresponds to the different phase difference. According to the principle of co-reflection, when the distance between FSS and antenna is an integral multiple of half wavelength, the reflected EM wave can be superimposed with the original EM wave to achieve the purpose of radiation enhancement. Therefore, by utilising the linear relationship between phase and frequency, the FSS structure can satisfy the co-reflection in UWB frequency range and achieve radiation enhancement.

The transmission characteristics of any periodic structure are closely related to the incident angle. The angular stability and polarisation stability have always been the bottleneck of the wideband FSS in practical engineering applications. The dispersion diagram can be used as an extremely effective approach in computing the performance of the FSS periodic structure. It reflects the relationship between the periodic unit reflection coefficient Γ and the propagation constant k_x. The dispersion diagrams of FSS1 at transverse electric (TE) mode and transverse magnetic (TM) mode are shown in Figs. 2*b* and *c* when the incident wave angle θ varies from 0° (*z*-axis) to 80° interval 10°. It can be seen from Figs. 2*b* and *c* that FSS1 exhibits stable broadband stop-band characteristics under both modes and wide-

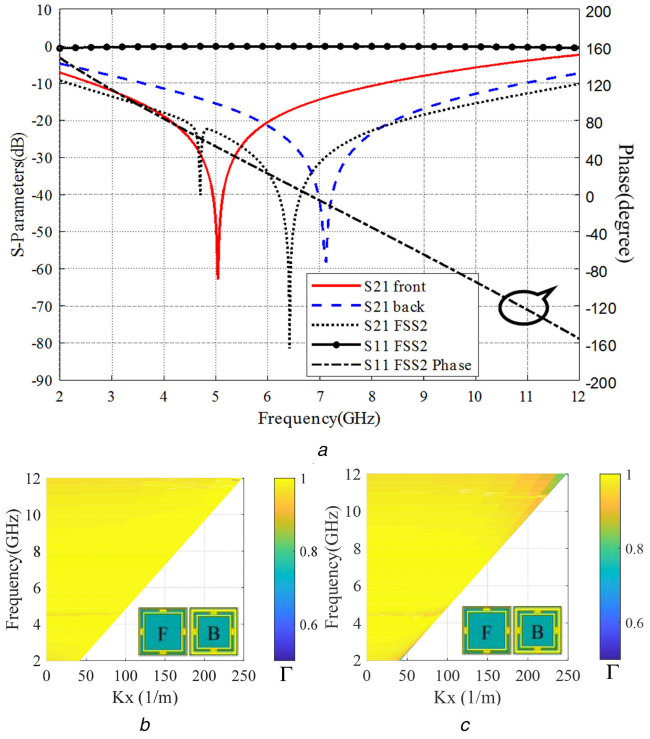

Fig. 3 *S-parameters and dispersion diagram of FSS2*
(a) S-parameters, ***(b)*** Dispersion diagram at TE mode, ***(c)*** Dispersion diagram at TM mode

angle incidence in the entire UWB operating band. As the angle is further increased, the FSS1 has a very narrow, weaker reflection region around 9 GHz at TE mode. This phenomenon may be because the square ring is slightly inferior to the circular ring in terms of polarisation stability and angular stability.

2.3 Miniaturised FSS2 design

To further reduce the reflector size without increasing the number of layers, some researchers have proposed a method of double-sided printing FSS. For example, the same FSS unit structure is printed on both sides of the signal-layer substrate with adding gap and branch loading [22], or printing completely different structural units on both sides within a combination of four diodes [23], or dislocating the upper and lower units for half a period [24]. In this paper, a more compact FSS reflector is designed by printing similar patterns (front and back) on both sides of a single-layer dielectric slab. The size of FSS2 is reduced by a quarter compared with the original structure. The structure and size of FSS2 are shown in Fig. 1*c* and Table 2, respectively.

With the same design idea and analysis method, the miniaturised FSS2 unit is designed and analysed. FSS2 can be regarded as a structure, in which two wide reflection bands separated by a certain thickness dielectric slab interact to realise UWB operation characteristics. In a sense, it can also be considered as a complementary FSS. It can be seen from Fig. 3*a* that the front structure of the miniaturised FSS2 guarantees low-frequency characteristics (2.6–8.2 GHz) and the back guarantee high-frequency characteristics (3.6–10.9 GHz). The combination of the two covers the entire UWB frequency. Similarly, it can be seen that the FSS2 unit has a high attenuation stop-band characteristic in the 2.2–12 GHz frequency band. At the same time, the phase changes linearly with the frequency, that is, the broadband radiation enhancement can be achieved when the antenna and FSS structure are fixed at a fixed distance.

The dispersion diagrams of FSS2 at TE mode and TM mode are shown in Figs. 3*b* and *c* when the incident wave angle θ varies from 0° (*z*-axis) to 80° interval 10°. It can be seen that FSS2 exhibits stable broadband stop-band characteristics under both modes in the entire UWB operating band.

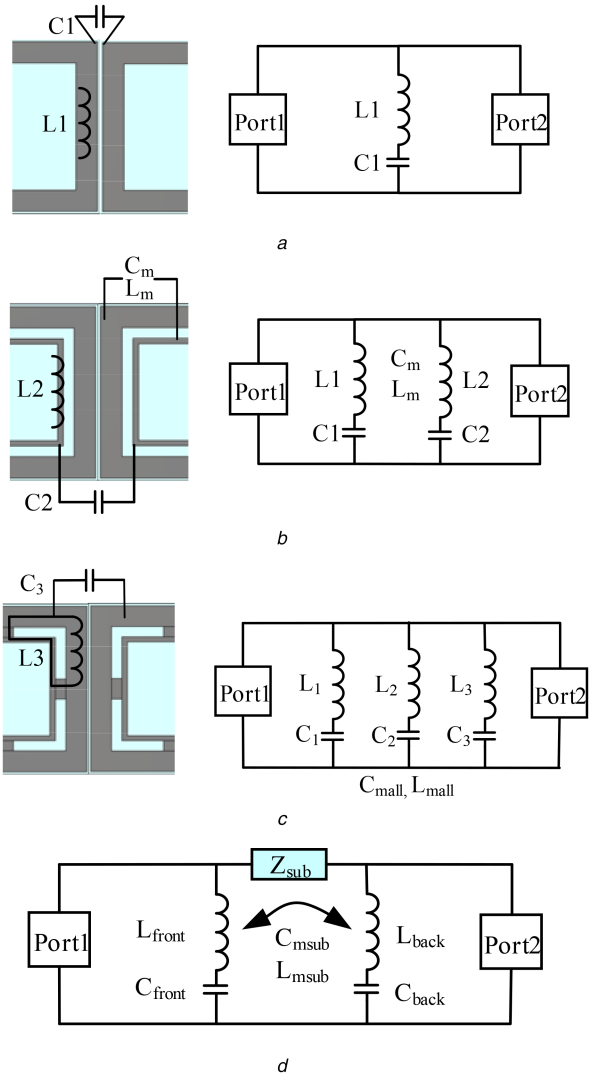

Fig. 4 *EC associated with FSS1 and FSS2*
(a) Outer of FSS1, ***(b)*** Outer and inner of FSS1, ***(c)*** FSS1, ***(d)*** FSS2

2.4 EC model

The EC model offers a simple and fast method in FSS analysis. The basic unit form of the designed FSS is a square loop, which can be equivalent to the inductor–capacitor series model [25, 26]. Fig. 4 shows the ECM of the designed FSSs. The equivalent inductance and capacitance of the circuit can be solved according to (1) and (2) [26], where *d*, *p*, *s*, and *g* are the dimensions of the square loop of FSSs in Table 2 and θ is the incidence angle.

The main advantage of the EC method is that the analysis speed is fast, but with the diversification of the design style, its main shortcomings such as the difficulty in extracting the circuit model and the poor calculation accuracy, are also very obvious, so it is more suitable for the previous performance estimation.

Fig. 4*a* shows the EC of the outer loop, where the loop contributes to inductance L_1 and the gap in between the two adjacent elements provides the capacitance C_1. Similarly, the inductance L_2 and capacitance C_2 of the inner loop is known. According to (1) and (2), inductance and capacitance values are $L_1 = 7.35\,\text{pH}$, $C_1 = 26.81\,\text{nF}$, $L_2 = 9.04\,\text{pH}$, and $C_2 = 40\,\text{pF}$, respectively. The resonance frequency calculated by the ECM is $f_1 = 5.45\,\text{GHz}$ and $f_2 = 13.1\,\text{GHz}$, and the corresponding EM simulation results are $f_{1S} = 4.95\,\text{GHz}$ and $f_{2S} = 9.70\,\text{GHz}$ (single simulation). The high resonance frequency deviation is larger than low frequency because the EC equations based on [25, 26] have limitations on the validity such as $w/p \ll 1$, $p/\lambda \ll 1$, and $p(1 + \sin\theta) < 1$. Owing to the influence of the mutual inductance L_m and mutual capacitance C_m between the inner and outer loops, the resonant frequency will have some offset, which corresponding

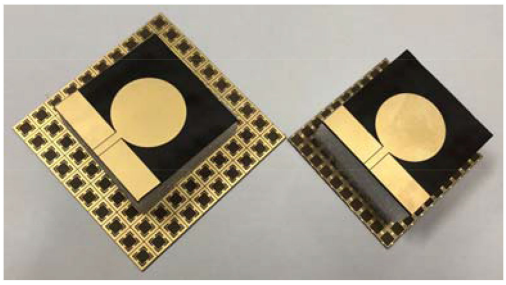

Fig. 5 *Photograph of the fabricated prototype antenna with FSS1 and FSS2*

$f'_{1S} = 4.37$ GHz and $f'_{2S} = 9.22$ GHz, respectively (S21 outer + inner in Fig. 2). After loading the branch, as shown in Fig. 4*c*, it is equivalent to adding a new resonant circuit, L_3C_3, whose resonant frequency will be between the two existing resonant frequencies. At the same time, the mutual inductance L_{mall} and mutual compatibility C_{mall} between multiple components of the entire structure can also become complicated. First, multiple L_3C_3 resonant circuits will produce lower transmission zero at the resonant frequency. Second, the branches connect the inner and outer loops to form the same reference plane. Third, to ensure that the TE and TM modes have the same characteristics, the branch structures also have a completely symmetrical characteristic. The above reasons will lead to broadband, single transmission zero effect (S21 FSS1 in Fig. 2). On the basis of the above method, as shown in Fig. 4*d*, the double-sided loaded FSS2 reflector structure can be regarded as a parallel connection of two single-pole series resonant circuits. The mutual coupling, L_{msub} and C_{msub}, between the two sides should also be considered. Since the thickness of the substrate is thin, its equivalent transmission line length can be neglected

$$\frac{X_L}{Z_0} = \omega L = \frac{d}{p}\cos\theta F(p,\ 2s,\ \lambda,\ \theta) \tag{1}$$

$$\frac{B_c}{Y_0} = \omega C = 4\frac{d}{p}\sec\theta F(p,\ g,\ \lambda,\ \theta)\varepsilon_{eff} \tag{2}$$

where

$$F(p,\ \omega,\ \lambda,\ \theta) = \frac{p}{\lambda}\left[\ln\left(\csc\frac{\pi\omega}{2p}\right) + G(p,\ \omega,\ \lambda,\ \theta)\right] \tag{3}$$

(see (4)) with

$$A_{\pm} = \frac{1}{\sqrt{\left[1 \pm (2p\sin\theta/\lambda) - (p\cos\theta/\lambda)^2\right]}} - 1 \tag{5}$$

$$\beta = \sin\left(\frac{\pi\omega}{2p}\right) \tag{6}$$

$$\varepsilon_{eff} = \frac{\varepsilon_r + 1}{2} - \frac{\varepsilon_r - 1}{2} \times \exp\left(\frac{-13h}{p}\right) - \left(\frac{100s^2}{d} - 2g + 10h\right) \tag{7}$$

2.5 Antenna loaded proposed FSSs

The antenna is installed at a distance h from the FSS reflector as indicated in Fig. 5. To enhance the antenna gain, the EM wave radiated by the antenna must be in phase with the EM wave reflected by the FSS reflector. Therefore, the phase of the EM wave of the antenna and the FSS reflector must satisfy the following equation [18]:

$$\phi_{fss} - 2\beta h = 2n\pi \quad n = \cdots -2,\ -1,\ 0,\ 1,\ 2,\ \ldots \tag{8}$$

Here, ϕ_{fss} is the reflection phase of the FSS; β is the propagation constant in the free space; and h is the height between the FSS and antenna. Taking the centre frequency 7 GHz and $\phi_{fss} = 0$, for example, h is calculated as 21.42 mm and $h = 22$ mm is chosen here. The FSS1 reflector uses 10×10 units, and the size is 82.5 mm × 82.5 mm. FSS2 uses the same number of cells, so the size is reduced by about 25% compared with FSS1.

To evaluate the UWB performance and gain enhancement of the designed FSSs, the comparison of the antenna with and without FSS are given in Fig. 6*a*. It can be seen that the average gain of the antenna is about 4.5 dBi without FSS loading, and gain variation is relatively large, about 4 dB. After loading FSS1, the average gain of the entire operating band is 8.5 dBi, and the gain variation is only 0.5 dB, which realises the gain enhancement and achieves the constant gain. This result is mainly due to the linear attenuation of the reflected phase of the FSS, which is equivalent to the linear change of the relative distance between the antenna radiator and the FSS reflector with the change of frequency. So, the EM wave radiated by the antenna and reflected by the FSS can be superimposed in the entire UWB frequency band and realise the antenna radiation enhancement. Similarly, FSS2 has the same properties. As can be seen from Fig. 6*a*, after loading miniaturised FSS2 reflector, the average gain decreases by 0.5 dB, and the gain variation remains within 0.5 dB. By losing a small portion of the gain in exchange for a significant reduction in the size of the FSS2, this compromise is necessary for some practical engineering application.

It can also be seen from Fig. 6*a* that the antenna gain enhancement effect is different at different frequencies, mainly because the radiation field distribution of the UWB antenna is significantly different at different frequencies. The results of some scholars have shown that the CPW-fed UWB antenna has large back-lobe energy at the low-frequency band, which is almost equivalent to the forward direction. After loading the designed FSS reflector, the back-lobe radiant energy is reflected and superimposed on the forward radiation field. Therefore, the gain enhancement in the low band is more obvious. With the increase of frequency, the CPW-fed UWB antenna gradually deforms the main radiation direction parallel to the antenna surface, which weakens the impact of FSS1 reflection on the antenna, so gain enhances relatively low at the high-frequency band.

The total efficiency of the UWB antenna with and without FSS reflectors is shown in Fig. 6*b*. The results show that, except for the low-end boundary of 3 GHz (maximum change, about 8%), the total efficiency of the antenna with and without FSS reflectors is almost equal over the whole operational band, both of which are >92%.

The existing research results show that the distance between the antenna and the reflector has a great influence on the antenna gain and working BW, especially on the working BW, and the gain is also affected by the size of the reflector. Taking FSS1, for example, Fig. 7 shows the reflection coefficient and maximum gain of the antenna with and without FSS1 at different distances. It should be noted that FSS2 acts on the antenna with the same law. It can be seen from Fig. 7*a* that with the distance increasing, the improvement of the reflection coefficient of the low-frequency band is more obvious, and the value is closer to the UWB antenna curve at the higher-frequency band. The main reason is that the main radiation direction of the CPW UWB antenna is perpendicular to the antenna plane at the low frequency, and the

$$G(p,\ \omega,\ \lambda,\ \theta) = \frac{1}{2} \times \frac{\left(1-\beta^2\right)^2\left[\left(1-(\beta^2/4)\right)(A_+ + A_-) + 4\beta^2 A_+ A_-\right]}{\left(1-(\beta^2/4)\right) + \beta^2\left(1+(\beta^2/2)-(\beta^4/8)\right)(A_+ + A_-) + 2\beta^6 A_+ A_-} \tag{4}$$

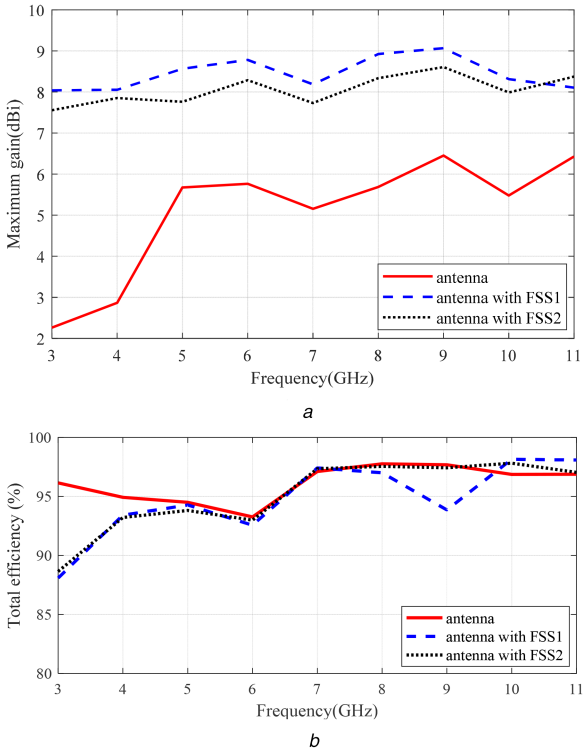

Fig. 6 *Maximum gain and total efficiency of the antenna with and without FSS1 and FSS2*

(a) Maximum gain, ***(b)*** Total efficiency

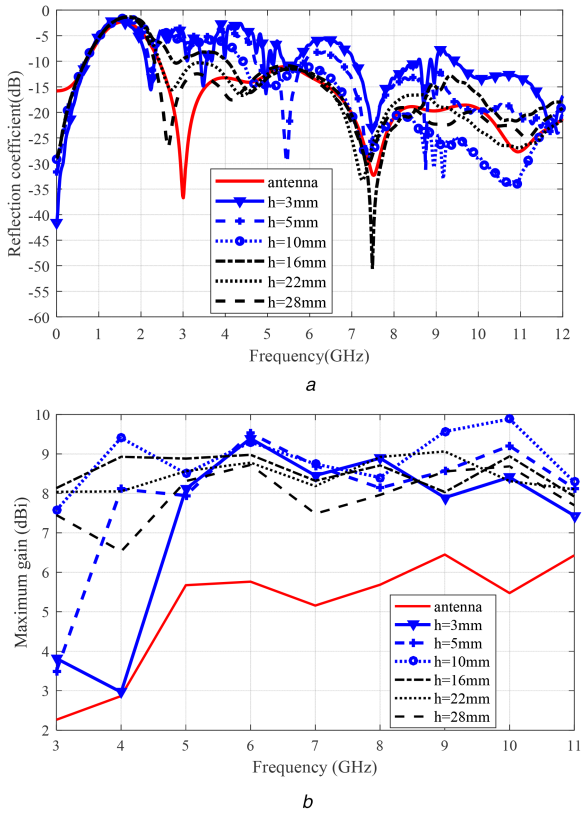

Fig. 7 *Reflection coefficient and maximum gain of the antenna with and without FSS1 at different h*

(a) Reflection coefficient, ***(b)*** Maximum gain

back lobe is relatively strong. It should be added that when the reflector is very close to the antenna such as $h = 3$ and 5 mm, the EM wave will form multiple strong reflections between them, which is reflected by the reflection coefficient jitter (or burred feature). In general, the closer the distance, the greater the gain enhancement, and vice versa. However, when $h = 3$ and 5 mm, the EM wave has multiple strong reflections between the antenna and reflector, which weakens the effect of gain enhancement. Especially when the frequency is low, the main radiation direction of the antenna is perpendicular to the antenna plane, and this adverse effect is more obvious. The result of Fig. 7*b* also proves this argument. In this paper, gain enhancement, gain variation, and reflection coefficients are balanced.

2.6 Time-domain analysis

One of the important applications of UWB antennas is high fidelity radiating and receiving time-domain pulse signal. To measure the influence of the designed reflector-loaded UWB antenna on the time-domain characteristics, two identical antennas were used as the receiving device (Rx) and transmitting device (Tx) to construct the time-domain simulation scene. The distance between the two antennas is 400 mm, which is four times the wavelength of the lowest operating frequency (3 GHz), which satisfies the far-field radiation conditions. The signal source uses a modulated Gaussian pulse, and the corresponding spectrum is 3.0–11 GHz. Fig. 8 shows the time-domain impulse response of the antenna with and without reflectors placed in parallel. The normalised amplitudes of the transmitted and received pulses are presented.

It can be seen from Fig. 8 that the received signal is very similar when the antenna with and without FSS reflectors, which means that the reflector does not distort the pulse. At the same time, the distortion of the pulse is quantitatively evaluated using the fidelity factor F [27]. This parameter reflects the cross-correlation between the transmitted signal and the received signal. The higher the cross-correlation, the better the signal fidelity. The fidelity calculation results of UWB antenna and antenna loading FSS1 and FSS2 are shown in Table 3. The fidelity factor for the three cases is >80%, and the general engineering application requirement is not <50%

$$F = \max_{\tau} \int_{-\infty}^{+\infty} \frac{S_{\mathrm{t}}(t)}{\| S_{\mathrm{t}}(t) \|_2} \cdot \frac{S_{\mathrm{r}}(t-\tau)}{\| S_{\mathrm{r}}(t) \|_2} \mathrm{d}t \tag{9}$$

where $S_{\mathrm{t}}(t)$ is the source pulse; $S_{\mathrm{r}}(t)$ is the received pulse; and τ is the time delay.

3 Experiment and analysis

Electronic printing technology is used to etch the FSS structure unit. Owing to the thinner dielectric plate, the designed structure is easily deformed during testing. To solve this problem, rigid foam is used as the solution, which is similar to air filling between the antenna and FSS reflector.

Fig. 9 shows simulated and measured reflection coefficients of the antenna with and without FSS1 and FSS2 reflector at the $h = 22$ mm in the entire UWB band. It can be seen that the simulated reflection coefficient in the entire UWB frequency band is lower than the industry standard −10 dB and the effects of FSS1 and FSS2 are consistent. It can be seen from Fig. 9 that the reflection coefficient is relatively large in the 2.5–4 GHz compared with the original antenna. The main reason is that the back-lobe radiation of the antenna in this band is large, and the EM field distribution is greatly affected after the reflector loading. Compared to the simulated result, the measured resonance point is entirely offset, which is mainly caused by the difference between the dielectric substrate parameters for simulation and testing, product processing error, and so on, but is in good agreement with the simulation result.

Figs. 10 and 11 show the radiation patterns in their principal radiating planes. The comparison of the results of the antenna with and without FSS reflectors clearly shows the effect of the designed UWB FSS reflectors on the UWB antenna. Both the reduction of the back lobe and the narrowing of the main lobe demonstrate that the FSS reflectors have a significant effect on antenna gain enhancement. At the same time, we can see that at the same distance, the two designed FSSs have similar performance in the designed frequency band, and the simulation results are consistent with the experimental measurements. The difference between them is mainly caused by the uniformity of the dielectric substrate, the

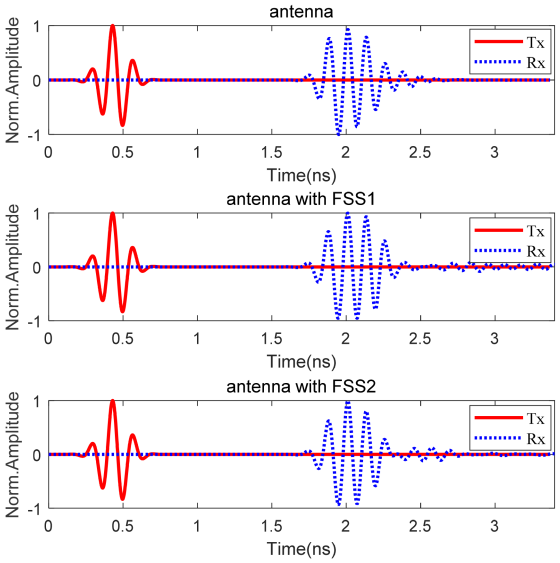

Fig. 8 *Tx and Rx signals of the antenna with and without FSSs*

Table 3 Fidelity factor

Fidelity factor		
Antenna	With FSS1	With FSS2
80%	81%	85%

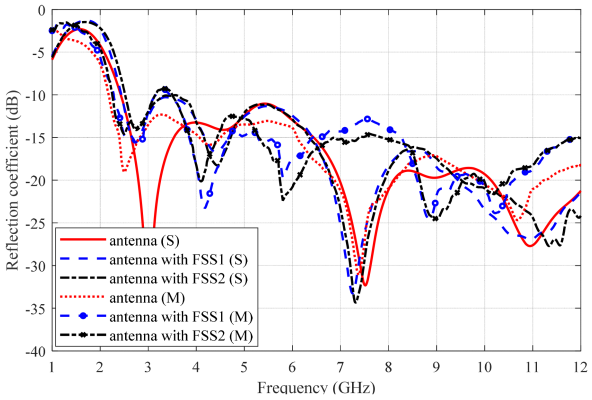

Fig. 9 *Simulated and measured reflection coefficient of the antenna with and without FSS1 and FSS2*

errors of the mechanical process, and the test environment. From Figs. 10 and 11, we can also see that the simulation results of the *xoz*-plane radiation pattern are consistent with measured results better than the *yoz*-plane. The *yoz*-plane forward radiation (90° direction) is better than the backward radiation (−90° direction, i.e. the feed point). The main reason for these results is that the influence of the subminiature version A radio-frequency connector is not taken into account during the simulation. The effects of FSS1 and FSS2 on the *xoz*-plane at 10 GHz are somewhat different. The main reason is that the main radiation direction of the antenna tends to be horizontal in the high frequency, not perpendicular to the antenna radiator. Therefore, if the FSS reflector below the antenna is too small, the effect of the radiation pattern is weak.

The main parameters of the UWB FSS loaded antenna are compared in Table 4. Compared to the two-layer, three-layer, or four-layer FSS designed in [4, 14, 17–19], the two FSSs proposed in this paper are all single-layer structures, which have the advantages of simple structure, low processing cost, small size, and small flatness in the band while satisfying the operating characteristics of UWB. On the premise that [20, 21] are consistent with the basic antenna used in this paper, the results of loading FSSs show that the proposed FSS improves the low-frequency characteristics of the antenna, the gain decreases by only 0.5 and 1 dB, while the size decreases by nearly 30 and 46%, and the gain flatness is still 0.5 dB. Therefore, the proposed two UWB FSSs

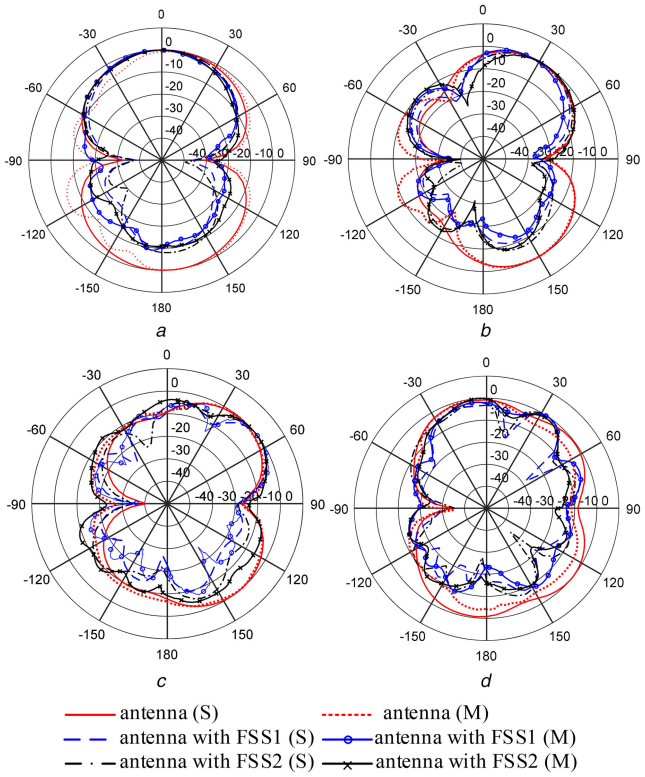

Fig. 10 *Simulated and measured yoz-plane (E-plane) radiation patterns of the antenna with and without FSS1, FSS2 at*
(a) 3 GHz, ***(b)*** 5 GHz, ***(c)*** 7 GHz, ***(d)*** 10 GHz

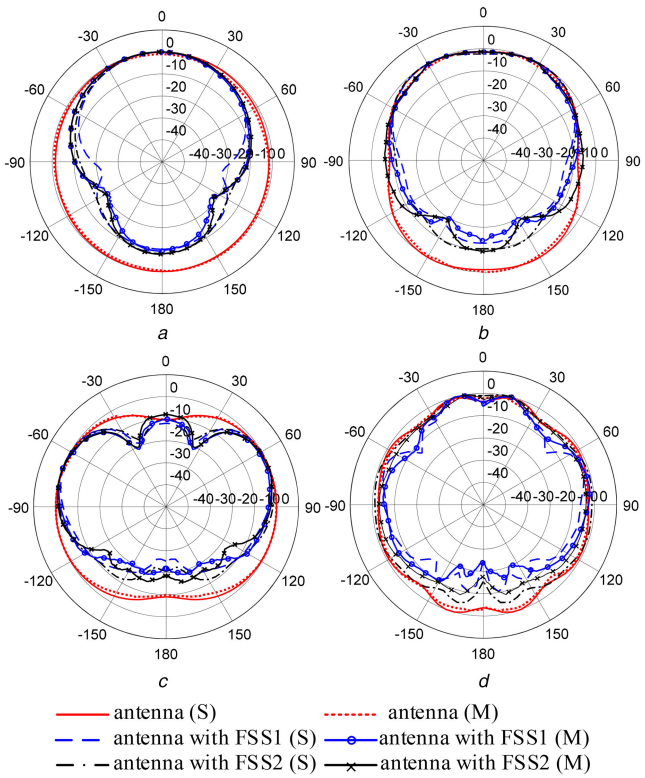

Fig. 11 *Simulated and measured xoz-plane (H-plane) radiation patterns of the antenna with and without FSS1, FSS2 at*
(a) 3 GHz, ***(b)*** 5 GHz, ***(c)*** 7 GHz, ***(d)*** 10 GHz

have compact shape, remarkable gain enhancement effect, and good gain variation. It should be noted that the high frequency in the table only takes into account 11 GHz.

Table 4 Comparison between the proposed antenna and previously proposed ones

	Unit dimensions, mm	BW, GHz	Gain, dBi	Variation, dB
[5]	115 × 115	3–11	8.0–9.5	0.75
[21]	115 × 115	3.4–11	8.5–9.5	0.5
[22]	115 × 115	3.4–11	8.5–9.5	0.5
FSS1	82.5 × 82.5	2.5–11	8.0–9.0	0.5
FSS2	62.5 × 62.5	2.5–11	7.5–8.5	0.5

4 Conclusion

In this paper, two compact UWB frequency selective surface reflectors are proposed for antenna gain enhancement application. The effectiveness of the proposed FSS reflectors is proved by using CPW-fed circular-disc monopole as a radiator. The larger FSS (8.25 mm × 8.25 mm) as antenna reflector obtains 8.5 dBi average gain, 0.5 dB gain variation, and 2.5–11 GHz operating BW. The more compact FSS by printing similar patterns on both sides of a single-layer dielectric slab realises a 25% size reduction and the same gain variation in the entire UWB frequency range. The experimental results are in good agreement with the simulation results, which proves the feasibility of our design method. With some parameter optimisation, the proposed FSSs can be applied to other UWB monopole antennas, and similar results can be obtained.

5 Acknowledgments

This work was supported in part by the research on high-efficiency miniaturised UWB array antenna (Science and Technology on High Power Microwave Laboratory), in part by the Realistic scene and high-precision navigation performance test and virtual test integrated simulation equipment (2017ZDXM-GY-117, key research and development plan of Shaanxi Province), and in part by the Xi'an Science and Technology Plan Project [2017080CG/RC043(XALG014), 2017080CG/RC043(XALG013), 2017080CG/RC043(XALG032)].

6 References

[1] First Report and Order: 'Revision of part 15 of the commission's rules regarding ultra-wideband transmission systems'. FCC 02-48, February 2002

[2] Liang, J., Guo, L., Chiau, C., *et al.*: 'Study of CPW-fed circular disc monopole antenna for ultra-wideband applications', *IEE Proc., Microw. Antennas Propag.*, 2005, **152**, (6), pp. 520–526

[3] Hu, M., Zhou, Y., Law, L., *et al.*: 'Study of a uniplanar monopole antenna for passive chipless UWB-RFID localization system', *IEEE Trans. Antennas Propag.*, 2010, **58**, (2), pp. 271–278

[4] Krishna, S., Kumar, R.: 'Slotted ground microstrip antenna with FSS reflector for high-gain horizontal polarisation'. *Electron. Lett.*, 2015, **51**, (8), pp. 599–600

[5] Yahya, R., Nakamura, A., Itami, M., *et al.*: 'A novel UWB FSS-based polarization diversity antenna', *IEEE Antennas Wirel. Propag. Lett.*, 2017, **16**, pp. 2525–2528

[6] Tao, Y., Li, B., Tang, M., *et al.*: 'Multi-layer tri-band frequency selective surface using stepped- and uniform-impedance resonators', *Electron. Lett.*, 2016, **52**, (8), pp. 583–585

[7] Lockyer, S., Vardaxoglou, C., Simpkin, A.: 'Complementary frequency selective surfaces', *IEE Proc., Microw. Antennas Propag.*, 2000, **147**, (6), pp. 501–507

[8] Joozdani, Z., Amirhosseini, K., Abdolali, A.: 'Wideband radar cross-section reduction of patch array antenna with miniaturised hexagonal loop frequency selective surface', *Electron. Lett.*, 2016, **52**, (9), pp. 767–768

[9] Lazaro, A., Ramos, A., Girbau, D., *et al.*: 'A novel UWB RFID tag using active frequency selective surface', *IEEE Trans. Antennas Propag.*, 2013, **61**, (3), pp. 1155–1168

[10] Akbari, M., Ali, M., Sebak, M., *et al.*: 'Spatially mutual coupling reduction between CP-MIMO antennas using FSS superstrate', *Electron. Lett.*, 2017, **53**, (8), pp. 516–518

[11] Bilal, M., Saleem, R., Shafique, F, *et al.*: 'An FSS based non-planar quad element UWB-MIMO antenna system', *IEEE Antennas Wirel. Propag. Lett.*, 2017, **16**, pp. 987–990

[12] Cho, S., Lee, H., Lee, G., *et al.*: 'Dual band frequency selective film design for indoor wireless LAN environment improvement'. 12th European Conf. Antennas and Propagation (EuCAP 2018), London, UK, April 2018, pp. 1–4

[13] Silva, M., Nóbrega, C., Silva, P., *et al.*: 'Stable and compact multiband frequency selective surfaces with Peano pre-fractal configurations', *IET Microw. Antennas Propag.*, 2013, **7**, (7), pp. 543–551

[14] Kundu, S., Chatterjee, A., Jana, S.K., *et al.*: 'A compact umbrella-shaped UWB antenna with gain augmentation using frequency selective surface', *Radio Eng.*, 2018, **27**, (2), pp. 448–454

[15] Barbagallo, S., Monorchio, A., Manara, G.: 'Small periodicity FSS screens with enhanced bandwidth performance', *Electron. Lett.*, 2006, **42**, (7), pp. 382–383

[16] Kern, J., Werner, H., Monorchio, A., *et al.*: 'The design synthesis of multiband artificial magnetic conductors using high impedance frequency selective surfaces', *IEEE Trans. Antennas Propag.*, 2005, **51**, (1), pp. 8–17

[17] Oli, T.: 'Design of a star shaped high gain UWB antenna using FSS for wireless communications'. Microwaves RF, June 2014, pp. 83–92

[18] Kushwaha, N., Kumar, R.: 'High gain UWB antenna using compact multilayer FSS'. IEEE Int. Microwave and RF Conf., Bangalore, India, 2014, pp. 100–103

[19] Ranga, Y., Matekovits, L., Weily, R., *et al.*: 'A constant gain ultra-wide band antenna with a multi-layer frequency selective surface', *Prog. Electromagn. Res. Lett.*, 2013, **38**, pp. 119–125

[20] Yahya, R., Nakamura, A., Itami, M.: 'Design of constant gain UWB planar antenna using FSS-based reflectors', *IEICE ComEx*, 2016, **5**, (1), pp. 27–32

[21] Yahya, R., Itami, M.: 'Design of constant gain UWB planar antenna using single-layer FSS'. IEEE Int. Symp. Antennas and Propagation USNC/URSI National Radio Science Meeting, Vancouver, BC, Canada, 2015, pp. 2015–2016

[22] Kushwaha, N., Kumar, R., Krishna, R.: 'Design and analysis of new compact UWB frequency selective surface and its equivalent circuit', *Prog. Electromagn. Res. C*, 2014, **46**, pp. 31–39

[23] Majidzadeh, M., Ghobadi, C., Nourinia, J.: 'Novel single layer reconfigurable frequency selective surface with UWB and multi-band modes of operation', *AEU-Int. J. Electron. C*, 2016, **70**, (2), pp. 151–161

[24] Dewani, A., O'Keefe, G., Thiel, V.: 'Transmission bandwidth enhancement using lateral displacement in a thin flexible single layer double side FSS'. 2015 Int. Symp. Antennas Propagation (ISAP), Hobart, TAS, Australia, 2015, pp. 1–4

[25] Langley, J., Parker, A.: 'Equivalent circuit model for arrays of square loops', *Electron. Lett.*, 1982, **18**, (7), pp. 294–296

[26] Hussain, T, Cao, S, Kayani, K, *et al.*: 'Miniaturization of frequency selective surfaces using 2.5-D knitted structures: design and synthesis', *IEEE Trans. Antennas Propag.*, 2017, **65**, (5), pp. 2405–2412

[27] Pancera, E., Zwick, T., Wiesbeck, W.: 'Spherical fidelity patterns of UWB antennas', *IEEE Trans. Antennas Propag.*, 2011, **59**, (6), pp. 2111–2119